Molecular Therapy
Oncology
Original Article

Nonsignaling extracellular spacer regulates tumor antigen selectivity of CAR T cells

Kelly T. Kennewick,[1,4] Yukiko Yamaguchi,[1,4] Jackson Gibson,[1] Ethan A. Gerdts,[1] Brook Jeang,[1] Dileshni Tilakawardane,[1] John P. Murad,[1] Wen-Chung Chang,[1] Sarah L. Wright,[1] Michalina S. Thiel,[1] Stephen J. Forman,[1,2] Lawrence A. Stern,[3] and Saul J. Priceman[1,2]

[1]Department of Hematology and Hematopoietic Cell Transplantation, City of Hope, Duarte, CA 91010, USA; [2]Department of Immuno-Oncology, Beckman Research Institute of City of Hope, Duarte, CA 91010, USA; [3]Department of Chemical, Biological, and Materials Engineering, University of South Florida, Tampa, FL 33620, USA

Advancing chimeric antigen receptor (CAR)-engineered T cells for the treatment of solid tumors is a major focus in the field of cellular immunotherapy. Several hurdles have hindered similar CAR T cell clinical responses in solid tumors as seen in hematological malignancies. These challenges include on-target off-tumor toxicities, which have inspired efforts to optimize CARs for improved tumor antigen selectivity and overall safety. We recently developed a CAR T cell therapy targeting prostate stem cell antigen (PSCA) for prostate and pancreatic cancers, showing improved preclinical antitumor activity and T cell persistence by optimizing the intracellular co-stimulatory domain. Similar studies were undertaken to optimize HER2-directed CAR T cells with modifications to the intracellular co-stimulatory domain for selective targeting of breast cancer brain metastasis. In the present study, we evaluate various nonsignaling extracellular spacers in these CARs to further improve tumor antigen selectivity. Our findings suggest that length and structure of the extracellular spacer can dictate the ability of CARs to selectively target tumor cells with high antigen density, while sparing cells with low antigen density. This study contributes to CAR construct design considerations and expands our knowledge of tuning solid tumor CAR T cell therapies for improved safety and efficacy.

INTRODUCTION

Chimeric antigen receptor (CAR) T cell therapy has demonstrated unprecedented clinical responses in patients with B cell malignancies, and efforts are under way to translate CAR T cell therapies for the treatment of solid tumors. However, CAR T cells have shown underwhelming clinical responses in solid tumors,[1,2] uncovering several challenges that must be overcome to develop safe and effective CAR T cell therapies for these diseases.[3–5] The success of CAR T cell therapy is contingent upon the combination of robust and durable antitumor activity and tumor specificity with minimal targeting of normal tissues. The highly restricted and uniform expression of B cell lineage markers CD19 and BCMA have been crucial in their clinical successes as CAR T cell therapies for hematological malignancies. Solid tumors lack such tumor-restricted targets, and CAR T cells for the treatment of solid tumors are directed to tumor-associated antigens that are commonly expressed on normal tissues. Adoptive transfer of solid tumor CAR T cells can therefore result in on-target off-tumor toxicities.[6,7] Therefore, designing tumor-selective CARs will be critical to the successes of solid tumor CAR T cells.

CARs consist of an antigen-binding domain, a nonsignaling extracellular spacer, and transmembrane and intracellular signaling domains, and the modular design of CARs has allowed rigorous optimization to improve potency and tumor antigen selectivity. Monoclonal antibody-derived single-chain variable fragment (scFv) is most used for antigen-binding domain, and many groups have performed affinity tuning of scFvs to discriminate tumors with high antigen expression from normal tissues with low antigen expression to minimize on-target off-tumor activities.[7–10] The intracellular co-stimulatory signaling domain with CD3ζ is crucial for inducing CAR T cell function upon antigen engagement. The choice of co-stimulatory domain affects the antigen density selectivity, persistence, and cytokine secretion of CAR T cells. CD28 and 4-1BB co-stimulatory domains are best characterized, and CD28 co-stimulatory domain is known to promote potent cytotoxicity, enabling superior sensitivity to low-density antigen expression, and 4-1BB favors CAR T cell persistence.[11–15]

We previously designed a prostate stem cell antigen-directed CAR (PSCA-CAR) comprising a humanized anti-PSCA scFv (A11 clone) tethered to a CD4 transmembrane domain via an extracellular immunoglobulin G (IgG)4-Fc spacer (void of the Fcγ receptor (FcγR)-binding CH2 domain) and an intracellular signaling domain consisting of 4-1BB co-stimulatory domain and CD3ζ cytolytic domain (PSCA(ΔCH2)BBζ).[12] This CAR, compared to a similar CAR construct containing a CD28 co-stimulatory domain (PSCA(ΔCH2)28ζ), showed improved overall *in vitro* and *in vivo* antitumor activity. Importantly, PSCA(ΔCH2)BBζ CAR T cells showed superior selectivity for tumor cells with higher PSCA expression relative to PSCA(ΔCH2)28ζ CAR T cells. However, PSCA(ΔCH2)BBζ CAR

Received 20 December 2023; accepted 27 February 2024;
https://doi.org/10.1016/j.omton.2024.200789.

[4]These authors contributed equally

Correspondence: Saul J. Priceman, Department of Hematology and Hematopoietic Cell Transplantation, City of Hope, Duarte, CA 91010, USA.
E-mail: spriceman@coh.org

T cells killed tumor cells with low PSCA expression *in vitro*, suggesting that further modifications to the construct may be warranted to avoid potential targeting of normal tissues with endogenous PSCA expression, including bladder, stomach, and colon.

Preclinical studies have showed that nonsignaling extracellular spacers can affect CAR T cell function,[16–19] and the domain can be modified to alter antitumor activity. For instance, spacers derived from endogenous receptors such as CD3ζ and CD28 enhance CAR T cell function by improving CAR stability in the membrane via interaction with endogenous proteins.[18,20] Extracellular spacers also lend flexibility and extracellular length to CARs and contribute to maintaining an optimal synapse necessary for antigen recognition. Flexible spacers such as IgG1 and IgG4 Fc enable access to sterically hindered antigens relative to rigid CD28- and CD8-derived spacers.[17,21,22] Moreover, the Fc region of IgG1 and IgG4 elicits FcγR-mediated immunogenicity, and IgG1- and IgG4-derived spacers have been further mutated to avoid this interaction and to improve CAR T cell persistence.[16,19,23] Although these previous reports have shown that the extracellular spacer domain contributes to overall CAR T cell functionality, little is known about its impact on tumor antigen selectivity.[24]

In this study, we varied the length and structure of the extracellular spacer domain in PSCA-BBζ and human epidermal growth factor receptor 2 (HER2)-BBζ CARs to evaluate the impact of this domain on tumor antigen selectivity of CAR T cells. We found that varying the spacer length and structure alters activation, cytokine secretion, proliferation, and tumor cell killing of CAR T cells following *in vitro* coculture of T cells and tumor cells with varying antigen density, as well as *in vivo* using human xenograft mouse models. Shortening the spacer domain led to CAR T cell selectivity toward target cells with high antigen density, sparing those with low antigen density. We identified a spacer that promotes potent, selective, and durable antitumor activity of CAR T cells against cells with high antigen expression. This study emphasizes the importance of evaluating the spacer domain when optimizing solid tumor CARs, and provides insights into engineering approaches to achieve robust and durable CAR T cell activity with improved tumor antigen selectivity.

RESULTS

Nonsignaling extracellular spacer affects tumor antigen sensitivity and function of PSCA-CAR T cells *in vitro*

To investigate the impact of the extracellular spacer length and to further optimize CAR T cell selectivity to high antigen density, we varied the spacer domain of PSCA-CARs with the 4-1BB co-stimulatory domain.[12] We tested 4 spacers: a 229-amino acid-long IgG4-Fc spacer with 2-point mutations (L235E; N297Q) in the CH2 domain (EQ), a 129-amino acid-long IgG4-Fc spacer with a deletion of the CH2 domain (ΔCH2), a 22-amino acid-long IgG4 hinge linker (HL) spacer with a deletion of the CH2-CH3 domains and a 10-amino acid-long synthetic spacer (L) (Figure 1A). T cells were transduced with lentivirus to express PSCA-CARs that varied in the extracellular spacer domain, and the molecular weight of respective PSCA-CARs was confirmed by western blotting (Figure 1B). All of the constructs contained the truncated CD19 (CD19t) as a marker of lentiviral transduction, and we demonstrated comparable transduction by CD19t expression (Figure 1C) and cell surface expression of PSCA-CARs by protein L staining (Figure 1D) using flow cytometry. All of the spacer variants of PSCA-CAR as well as untransduced (UTD) control T cells had similar CD4/CD8 ratios (CD4 34.5% ± 1.36% SEM, CD8 65.5% ± 1.36% SEM), and *ex vivo* expansion of PSCA-CAR T cells was also comparable (Figure 1E).

We next assessed CAR T cell function using *in vitro* tumor cell killing assays by coculturing CAR T cells with the prostate cancer cells PC3 and DU145, engineered to express high antigen density PSCA under the EF1a promoter (PC3-PSCA^{hi}, DU145-PSCA), along with PC3 cells engineered to express PSCA under the control of an attenuated promoter (PGK100) to generate cells with low antigen density (PC3-PSCA^{lo}) (Figures 2A and 2B). T cell activation was measured by protein expression of CD137 by flow cytometry, and interferon γ (IFN-γ) secretion was quantified by ELISA after 24 h. All PSCA-CAR T cell variants showed robust activation against DU145-PSCA and PC3-PSCA^{hi} tumor cells (Figure 2C). PSCA-CAR T cells containing EQ and ΔCH2 (PSCA(EQ), PSCA(ΔCH2)) showed high CD137 expression against tumor cells regardless of antigen density, albeit a lower CD137 mean fluorescence intensity (MFI) against PC3-PSCA^{lo} cells (Figure 2D). However, PSCA-CAR T cells with HL and L spacers significantly reduced both the frequency and cell-surface density of CD137 in the presence of tumor cells with low antigen density, suggesting their greater selectivity for tumor cells with high antigen density. IFN-γ production by EQ, ΔCH2, and HL-containing PSCA-CAR T cells against DU145-PSCA and PC3-PSCA^{hi} cells was robust, yet only EQ- and ΔCH2-containing PSCA-CAR T cells produced measurable IFN-γ against PC3-PSCA^{lo} tumors (Figure 2E). We next stimulated PSCA-CAR T cells with varying concentrations of plate-bound recombinant human PSCA protein, against observing that only EQ- and ΔCH2-containing PSCA-CAR T cells produced robust IFN-γ in response to recombinant PSCA protein below 1.25 μg/mL (Figure 2F). L-containing PSCA-CAR T cells failed to produce IFN-γ regardless of tumor antigen density, despite their activation in response to tumor cells with high antigen density (Figures 2C–2F). Varying only the nonsignaling extracellular spacers in the PSCA-CAR resulted in differences in CD137 expression and IFN-γ production, providing evidence that this domain has the potential to affect the function of CAR T cells, and that shortening the spacer length enhances tumor antigen selectivity.

We next evaluated whether these differences in T cell activation translate into differences in tumor cell killing by coculturing PSCA-CAR T cell variants with PC3 tumor cells with low or high antigen density at an effector-to-tumor (E:T) ratio of 1:20 in long-term assays. All of the spacer variants demonstrated potent and comparable cytotoxicity against PC3-PSCA^{hi} tumor cells, but cytotoxicity against PC3-PSCA^{lo} tumor cells varied among the spacer variants (Figures 3A and 3B). While PSCA-CAR T cells with EQ and ΔCH2 demonstrated robust tumor cell killing independent of antigen density, the HL- and

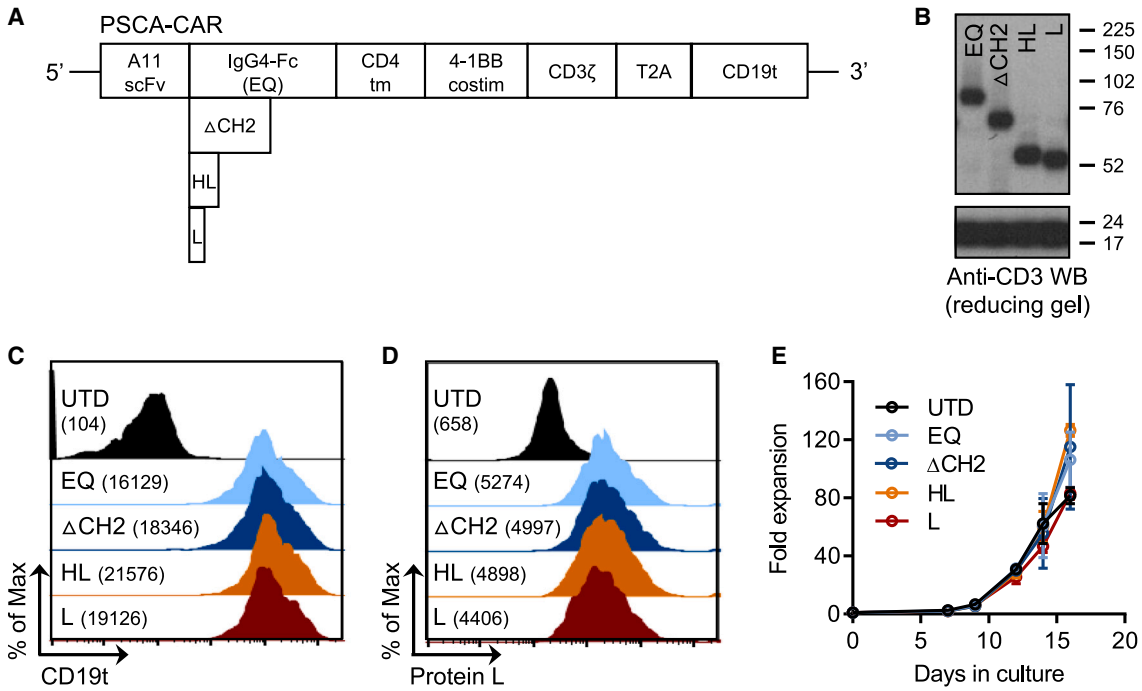

Figure 1. PSCA-CAR T cells containing varying nonsignaling extracellular spacers

(A) Diagram of the lentiviral expression cassette with PSCA-CARs containing the humanized scFv (A11 clone) targeting PSCA, a CD4 transmembrane domain, a cytoplasmic 4-1BB co-stimulatory domain, and a cytolytic CD3ζ domain. The nonsignaling extracellular spacer domain was altered to be either a 229-amino acid-modified human IgG4 Fc spacer with a double mutation (L235E; N297Q) within the CH2 region (EQ), a 129-amino acid-modified human IgG4 Fc spacer (void of the CH2 domain, ΔCH2), a 22-amino acid IgG4 HL, or a 10-amino acid synthetic linker (L). A nonsignaling CD19t, separated from the CAR with a T2A ribosomal skip sequence, was expressed as a surrogate marker of transduction. (B) Molecular weight of CARs with varying spacer length detected by western blotting CD3ζ protein. Endogenous T cell receptor was also detected (17–24 kDa). (C) UTD and PSCA-CAR T cells containing either EQ, ΔCH2, HL, or L spacers were evaluated by flow cytometry for CD19t expression to detect lentiviral transduction of CARs. (D) Protein L binding was evaluated by flow cytometry to detect cell surface expression of the scFv of the CAR. (E) *Ex vivo* expansion kinetics for UTD and PSCA-CAR T cells over 16 days in culture. All of the data are representative of at least 2 independent experiments with at least 2 donors.

L-containing PSCA-CAR T cells showed significantly reduced killing of PC3-PSCA^{lo} tumor cells, consistent with the trends in reduced CD137 expression and IFN-γ production in response to low antigen density. Despite the potent cytotoxicity against PC3-PSCA^{hi} cells, only EQ-, ΔCH2-, and HL-containing CAR T cells expanded following coculture. None of the spacer variants were able to expand in coculture with PC3-PSCA^{lo} tumor cells, even though PSCA-CAR T cells with EQ and ΔCH2 were able to kill these cells (Figure 3C). We also evaluated programmed cell death protein 1 (PD-1) induction as a measure of T cell exhaustion, and surprisingly, PSCA-CAR T cells with HL showed significantly lower induction of PD-1 than those with EQ and ΔCH2 spacers despite their similar activation and proliferation (Figure 3D). Taken together, these results suggest that the nonsignaling extracellular spacer affects tumor antigen sensitivity and function of CAR T cells.

Nonsignaling extracellular spacer affects tumor antigen sensitivity and function of HER2-CAR T cells *in vitro*

To extend these findings to other CAR targets, we evaluated HER2-directed CAR (HER2-CAR) T cells with respect to the impact of the spacer length on activation and tumor cell killing. We used the same spacer variants in HER2-CARs comprising a humanized anti-HER2 scFv (4D5 clone) tethered to a CD8 transmembrane domain and a 4-1BB co-stimulatory domain[14] (Figure 4A). All of the HER2-CAR designs demonstrated comparable transduction evaluated by cell surface expression of CD19t and CAR (Figures 4B and 4C), as well as *ex vivo* expansion (Figure 4D); however, the presence of a ΔCH2 spacer resulted in lower cell surface density measured by protein L staining, suggesting reduced expression stability of this HER2-CAR construct (Figure 4C).

To assess the *in vitro* functionality of these HER-CAR T cells, we used breast cancer lines with varying levels of endogenous or engineered HER2 expression measured by flow cytometry (HER2^{-} MDA-MB-468 cells, low HER2-expressing MDA-MB-361 and MDA-MB-231BR [231BR] cells, and high HER2-expressing BBM1 cells and MDA-MB 231BR cells engineered to overexpress HER2 [231BR-HER2]) (Figure 4E). We found that all of the HER2-CAR T cell variants produced IFN-γ against MDA-MB 231BR-HER2 and BBM1 cells with abundant HER2 expression, but levels of IFN-γ were significantly lower in HER2-CAR T cells containing HL and L spacers relative to those with EQ spacers (Figure 4F). HER2-CAR T cells with HL

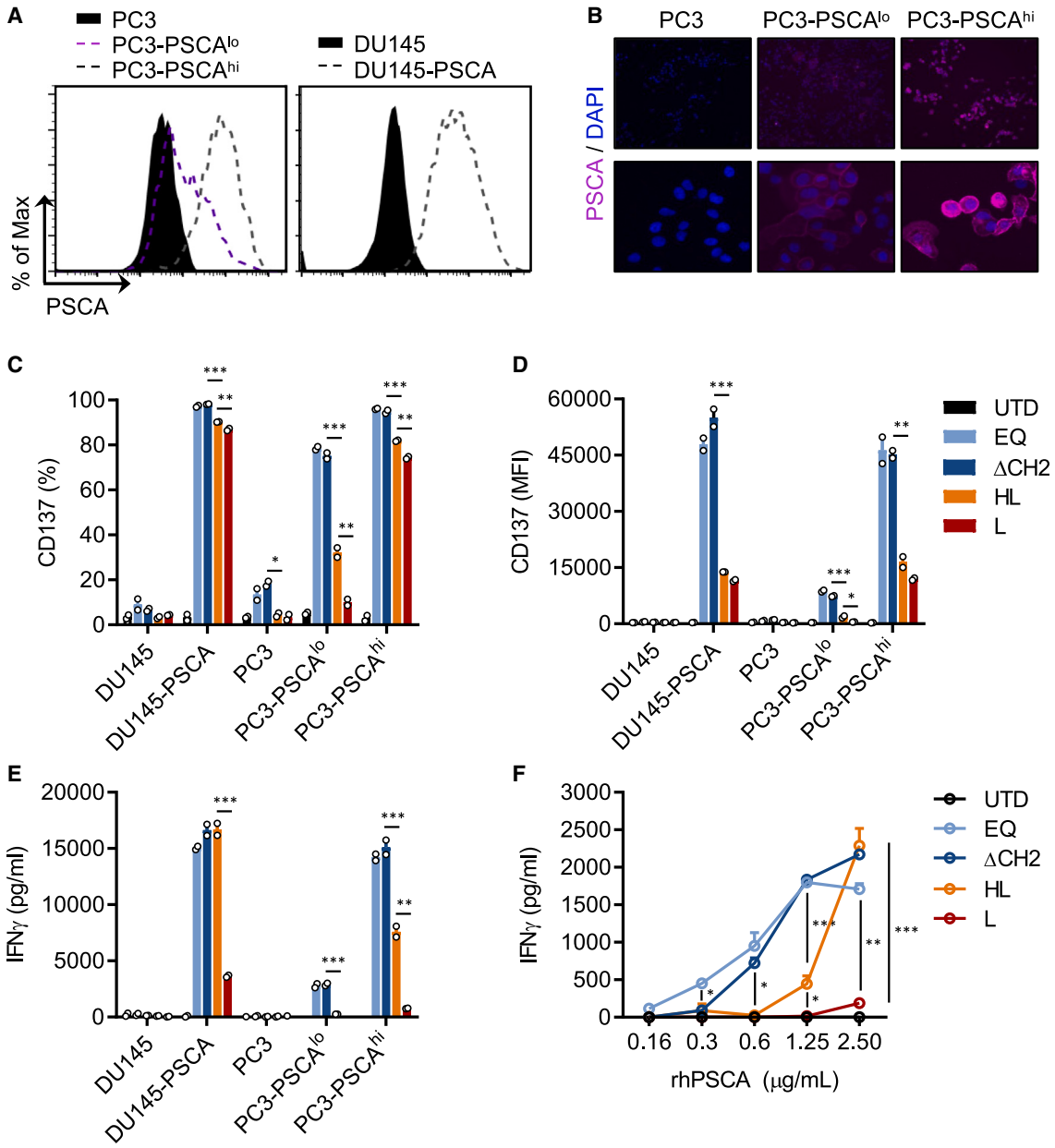

Figure 2. Nonsignaling extracellular spacer regulates antigen sensitivity and functionality of PSCA-CAR T cells *in vitro*

(A) Flow cytometry analysis of PSCA expression in lentivirally transduced human prostate cancer cell lines PC3 and DU145. (B) Fluorescence microscopy analysis of PSCA expression in PC3, PC3-PSCA^{lo}, and PC3-PSCA^{hi} tumor cells. (C and D) Percentage (C) and MFI (D) of CD137 expression in UTD and PSCA-CAR T cells containing either EQ, ΔCH2, HL, or L spacers. CD137 expression was evaluated by flow cytometry following 24-h coculture with the indicated tumor targets at a 1:2 E:T ratio. (E) IFN-γ production quantified by ELISA in supernatants from UTD or indicated PSCA-CAR T cells cultured overnight with tumor targets at a 1:1 E:T ratio. (F) IFN-γ production quantified by ELISA in supernatants from UTD or indicated PSCA-CAR T cells cultured overnight on plate-bound recombinant human PSCA at varying protein concentrations. All of the data are representative of at least 2 independent experiments performed with duplicates with at least 2 donors. Mean ± SEM is presented with p value (*$p < 0.05$, **$p < 0.01$, ***$p < 0.001$).

and L spacers did not produce IFN-γ when cocultured with MDA-MB-361 and 231BR tumor cells with low HER2 expression, suggesting the selectivity of HL- and L-containing HER2-CAR T cells to tumors with higher antigen density. This trend in IFN-γ secretion was further confirmed by stimulating HER2-CAR T cells with varying concentrations of plate-bound recombinant human HER2 protein (Figure 4G). We also assessed tumor cell killing in coculture assays by flow cytometry and found that all of the HER2-CAR T cell variants

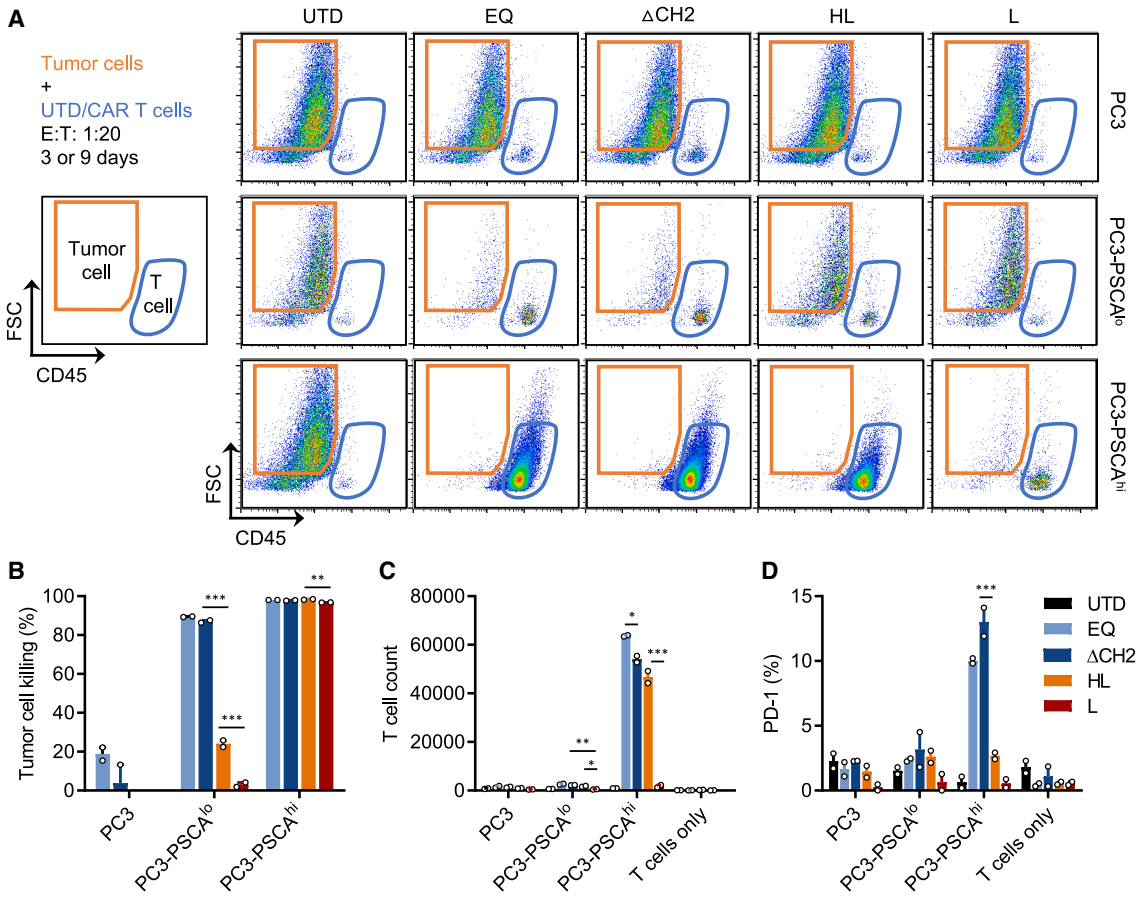

Figure 3. Short extracellular spacers improve selectivity of PSCA-CAR T cells to prostate tumor cells with higher antigen density

UTD and PSCA-CAR T cells containing either EQ, ΔCH2, HL, or L spacers were cocultured with PC3, PC3-PSCA^{lo}, and PC3-PSCA tumor cells at a 1:20 E:T ratio, and flow cytometry analysis was performed after 9 days. (A) Representative flow cytometry plots comparing the spacer variants. Gating strategy to distinguish tumor cells and T cells (left). (B–D) Quantification of tumor cell killing (B), T cell expansion (C), and PD-1 expression (D). Tumor cell killing was normalized to respective conditions containing control UTD T cells. PD-1 expression was assessed in CAR T cells detected by CD19t expression. All of the data are representative of at least 2 independent experiments performed with duplicates with at least 2 donors. Mean ± SEM is presented with p value (*$p < 0.05$, **$p < 0.01$, ***$p < 0.001$).

potently killed BBM1 and 231BR-HER2 cells (Figure 4H). Although HER2-CAR T cells with EQ spacer showed robust killing of MDA-MB-361 and 231BR tumor cells, HER2-CAR T cells with HL and L spacers did not kill these tumor cells with low antigen density. Taken together, these results indicate selectivity of HL- and L-containing HER2-CAR T cells to high antigen density similar to that of PSCA-CAR T cells. Although both HL- and L-containing HER2-CAR T cells were selective to tumor cells with abundant antigen expression, the HL spacer allowed for superior tumor killing and IFN-γ secretion compared with the L spacer, suggesting that extracellular spacer length can regulate CAR T cell function.

Nonsignaling extracellular spacer affects tumor antigen sensitivity and efficacy of PSCA-CAR T cells *in vivo*

The presence of the HL spacer in both PSCA- and HER2-CAR T cells resulted in improved selectivity for tumor cells with high antigen density. We next evaluated the impact of spacer length on the *in vivo* therapeutic activity of PSCA-CAR T cells. We subcutaneously engrafted PC3-PSCA^{hi} cells in one flank and PC3-PSCA^{lo} cells in the opposite flank of male NSG mice, and adoptively transferred 5×10^6 PSCA-CAR T cells with ΔCH2, HL, or L spacers by intravenous (i.v.) injection (Figure 5A). Regardless of the spacer, mice that received PSCA-CAR T cells showed potent growth inhibition of PC3-PSCA^{hi} tumors (Figures 5B and 5D). Although ΔCH2-containing PSCA-CAR T cells managed to control the growth of PC3-PSCA^{lo} tumors, PSCA-CAR T cells with HL and L spacers showed minimal antitumor activity against these tumors (Figures 5C and 5E). Furthermore, despite the durable antitumor activity of PSCA-CAR T cells with ΔCH2 and HL spacers against PC3-PSCA^{hi} tumors, L-containing PSCA-CAR T cells failed to show similar therapeutic activity (Figures 5B and 5D). These results reproduced the trend we observed *in vitro*, with PSCA-CAR T cells with the HL spacer demonstrating the greatest potency and selectivity for tumors with high tumor antigen density *in vivo*.

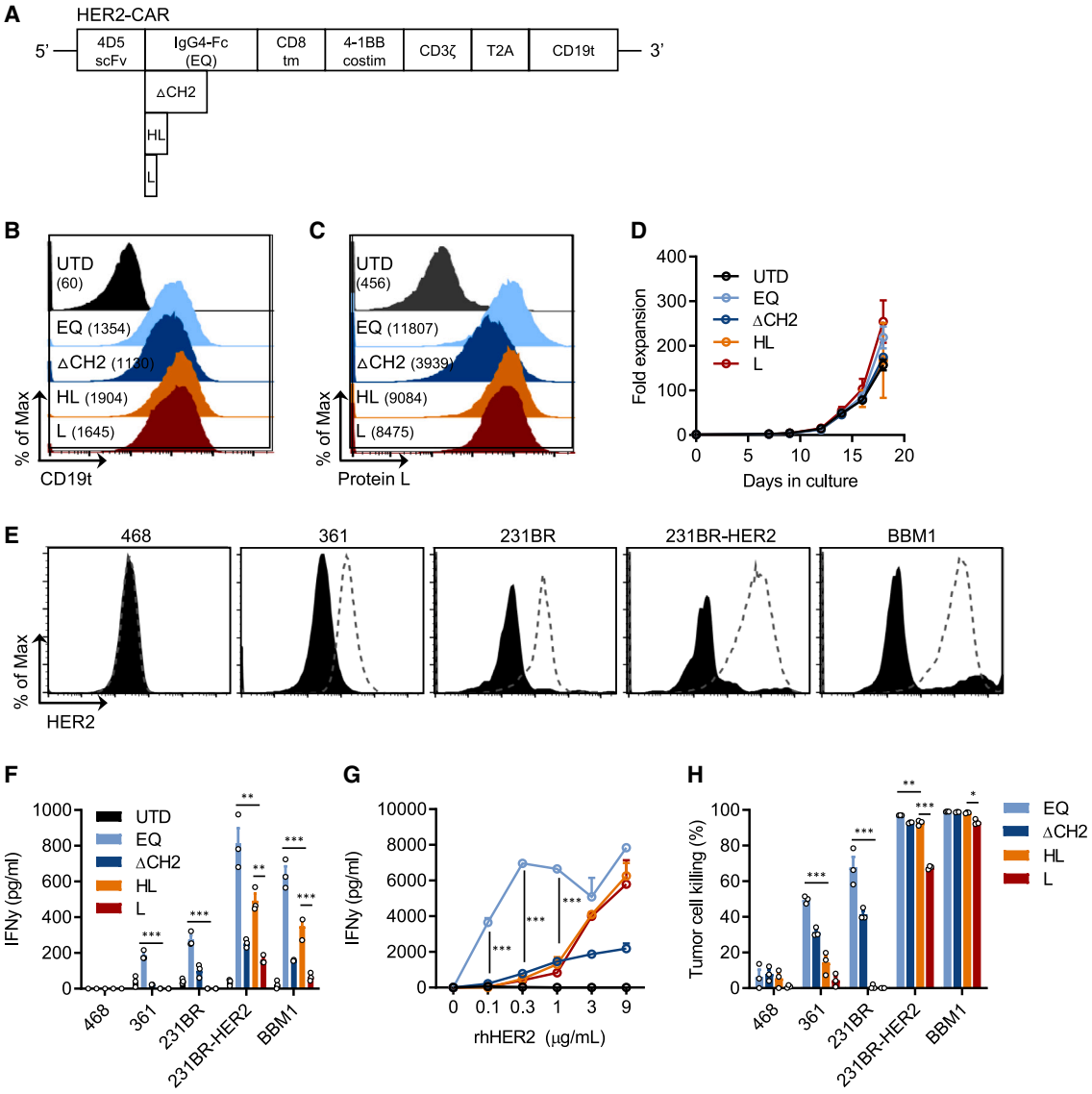

Figure 4. Nonsignaling extracellular spacer controls antigen sensitivity and functionality of HER2-CAR T cells *in vitro*

(A) Diagram of the lentiviral expression cassette with HER2-CARs containing the humanized scFv (4D5 clone) targeting HER2 with a CD8 transmembrane domain, a cytoplasmic 4-1BB co-stimulatory domain, and a cytolytic CD3ζ domain. The nonsignaling extracellular spacer domain was altered to be either a 229-amino acid-modified human IgG4 Fc spacer with a double mutation (L235E; N297Q) within the CH2 region (EQ), a 129-amino acid-modified human IgG4 Fc spacer (void of the CH2 domain, ΔCH2), a 22-amino acid IgG4 HL, or a 10-amino acid synthetic linker (L). A nonsignaling CD19t, separated from the CAR with a T2A ribosomal skip sequence, was expressed as a surrogate marker of transduction. (B) UTD and HER2-CAR T cells containing either EQ, ΔCH2, HL, or L spacers were evaluated by flow cytometry for CD19t expression to detect lentiviral transduction of CARs. (C) Protein L binding was evaluated by flow cytometry to detect cell surface expression of the scFv of the CAR. (D) *Ex vivo* expansion kinetics for UTD and PSCA-CAR T cells over 18 days in culture. All of the data are representative of at least 2 independent experiments. (E) Flow cytometric analysis of HER2 expression in human breast cancer cell lines. HER2-MDA-MB-468 (468), MDA-MB-361 (361), MDA-MB-231BR (231BR), and MDA-MB-231BR cells engineered to overexpress HER2 (231BR-HER2), and BBM1 tumor cells have varying HER2 expression. (F) IFN-γ production quantified by ELISA in supernatants from UTD or indicated HER2-CAR T cells cocultured overnight with tumor targets at a 1:1 E:T ratio. (G) IFN-γ production quantified by ELISA in supernatants from UTD or indicated HER2-CAR T cells cultured overnight on plate-bound recombinant human HER2-Fc at varying protein concentrations. (H) Tumor cell killing by HER2-CAR T cells. HER2-CAR T cells containing either EQ, ΔCH2, HL, or L spacers were cocultured with indicated tumor cells at a 1:20 E:T ratio, and flow cytometry analysis was performed after 8 days. Tumor cell killing was calculated by normalizing to respective conditions containing control UTD T cells. All of the data are representative of at least 2 independent experiments performed with duplicates or triplicates with at least 2 donors. Statistical analysis was performed to compare EQ, HL, and L spacers. Mean ± SEM is presented with p value (*$p < 0.05$, **$p < 0.01$, ***$p < 0.001$).

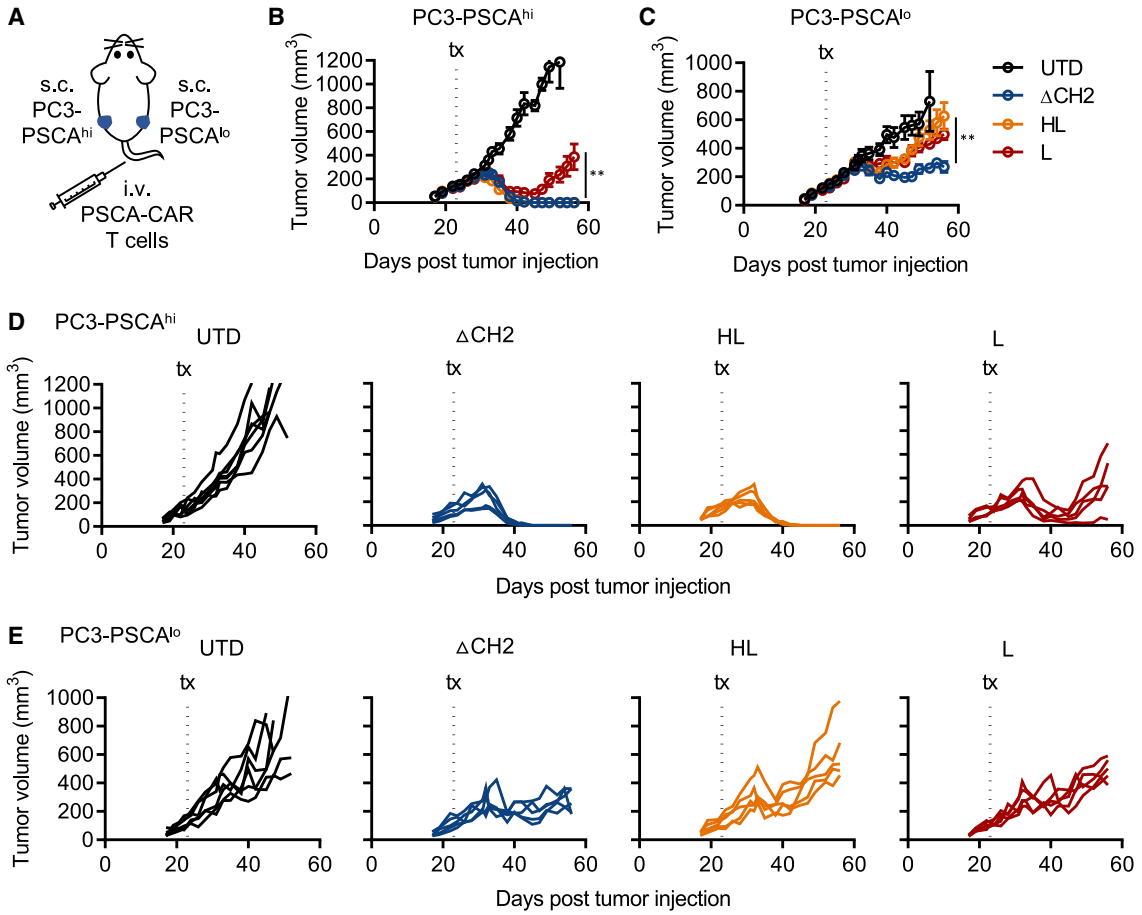

Figure 5. Short extracellular spacers in PSCA-CAR T cells promote selective killing of prostate cancer cells with high antigen density *in vivo*

(A) Illustration of *in vivo* model. Male NSG mice bearing subcutaneous PC3-PSCA^{hi} and PC3-PSCA^{lo} tumor cells (2.5×10^6 each site) on either flank with treated with 0.5 M Mock or indicated PSCA-CAR T cells by i.v. injection on day 22. (B–E) Average and individual tumor volumes (mm^3) of PC3-PSCA^{hi} (B and D) and PC3-PSCA^{lo} (C and E) tumors. All of the data are representative of at least 2 independent experiments with at least 2 donors. Each group had N ≥ 5. Statistical significance shown indicates results of ANOVA performed on 56 days posttumor injection. Mean ± SEM is presented with p value (*$p < 0.05$, **$p < 0.01$, ***$p < 0.001$).

We validated our findings using the human pancreatic adenocarcinoma (HPAC) model that expresses high levels of endogenous PSCA (Figure 6A). ΔCH2-, HL-, and L-containing PSCA-CAR T cells were statistically different in HPAC tumor cell killing using *in vitro* coculture assays (Figure 6B). In mice bearing subcutaneous HPAC tumors, potent antitumor activity was observed with PSCA-CAR T cells containing ΔCH2 and HL spacers, with heterogeneous responses with L-containing PSCA-CAR T cells (Figures 6C and 6D). Moreover, the trend in antitumor activity among PSCA-CAR T cells correlated with the abundance of tumor-infiltrating PSCA-CAR T cells in HPAC tumors (Figures 6E–6G) and circulating PSCA-CAR T cells in peripheral blood (Figure 6H), suggesting their varying ability to traffic to and proliferate in HPAC tumors. Overall, these data support the differential antitumor activity of CAR T cells against tumors with varying antigen density through the nonsignaling extracellular spacer.

DISCUSSION

On-target-off-tumor-toxicities are a major concern in the development of solid tumor-directed CAR T cells. Many studies have shown that modifications to the scFv, transmembrane, and intracellular signaling domains alter the antigen sensitivity of CARs, and optimizing these domains can improve the tumor selectivity of CAR T cells. We previously developed PSCA- and HER2-CAR T cells that demonstrated durable antitumor activity against target cells, including those with low and high antigen density. In this study, we further modulated these CAR designs to show that varying the nonsignaling extracellular spacer domain length and structure can improve the tumor selectivity of CAR T cells. Importantly, we left all of the other domains in the CAR construct constant while focusing exclusively on the impact of modifying the nonsignaling extracellular spacer domain on CAR T cell function and tumor selectivity. Our data using two different CAR targets show that in contrast to the

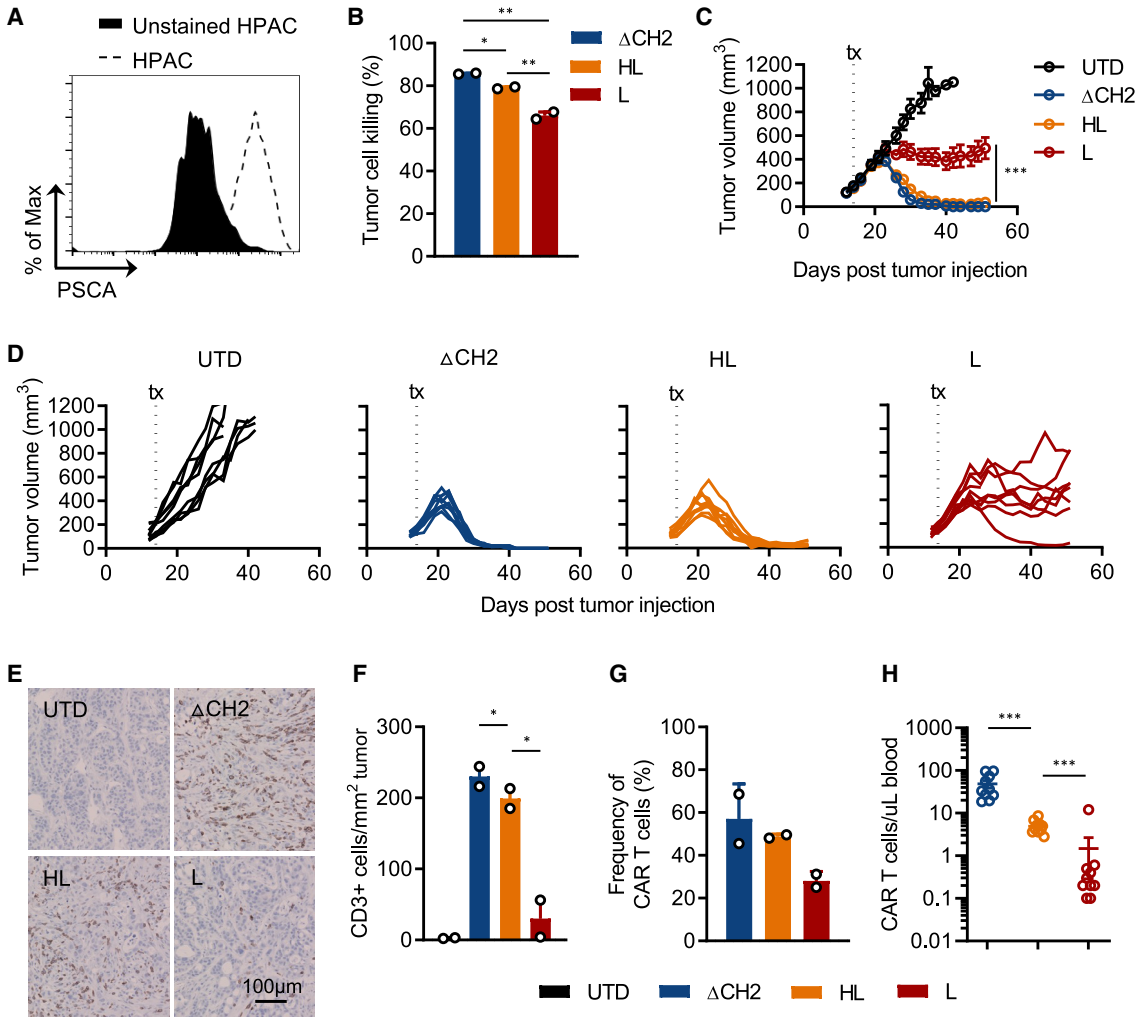

Figure 6. Nonsignaling extracellular spacer regulates antitumor activity of PSCA-CAR T cells against pancreatic ductal adenocarcinoma *in vivo*

(A) PSCA expression in HPAC cells evaluated by flow cytometry. (B) Quantification of tumor cell killing by PSCA-CAR T cells containing either ΔCH2, HL, or L spacers following a 3-day coculture with PSCA$^+$ HPAC tumor cells at a 1:1 E:T ratio. (C and D) Average (C) and individual (D) tumor volumes (mm^3) in NSG mice bearing subcutaneous HPAC (2.5×10^6) tumors on day 0, and treated with 5 M UTD or indicated PSCA-CAR T cells by i.v. injection on day 16. Statistical significance shown indicates results of ANOVA performed on 51 days posttumor injection. (E) Immunohistochemistry staining of human CD3 in HPAC tumors from mice treated with UTD or PSCA-CAR T cells containing either ΔCH2, HL, or L spacers. (F) Quantification of CD3$^+$ human T cells per unit area of HPAC tumors stained by immunohistochemistry. (G) Frequency of CAR T cells relative to the total cells in HPAC tumors measured by flow cytometry. (H) Concentration of circulating CAR T cells in peripheral blood measured by flow cytometry. All of the data are representative of at least 2 independent experiments with at least 2 donors. *In vitro* tumor killing assays were performed with duplicates (B). *In vivo* studies were performed with N = 10 per group. Circulating CAR T cells were quantified in all of the mice (H). Tumor was harvested from 2 mice (E–G), and tumor volume is shown with N = 8 (A and B). Mean ± SEM is presented with p value (*p < 0.05, **p < 0.01, ***p < 0.001).

longer IgG4 spacer domains, the 22-amino acid HL spacer resulted in selective antitumor activity against target cells with high antigen density while sparing those with low antigen density. We assessed the *in vivo* antitumor activity of PSCA-CAR T cells in mice bearing subcutaneous human prostate and pancreatic tumors and demonstrated potent and selective antitumor activity of PSCA(HL)-CAR T cells *in vivo* for tumors with higher antigen density, as compared with the longer spacer-containing PSCA-CAR T cells. The presence of the synthetic short L spacer hampered IFN-γ production and proliferation, with dampened overall antitumor function of CAR T cells *in vitro* and *in vivo* regardless of antigen density, suggesting that a nonstructural short spacer is inadequate for eliciting robust antitumor activity. Taken together, these findings highlight the importance of optimizing the spacer domain to develop effective solid tumor CAR T cell therapies with reduced potential for on-target off-tumor toxicities in normal tissue with low target expression. This study not only supports that the spacer domain modulates the antitumor activity of CAR T cells[16–23] but also identifies the spacer domain as a regulator to adjust the sensitivity of CAR T cells to target antigen density.

Previous studies have suggested that long spacers may provide sufficient length and flexibility necessary for binding epitopes proximal to the cell membrane, and short spacers may be more suitable for CAR binding epitopes distal to the cell membrane.[21,25–27] HER2 has large extracellular domains, and the trastuzumab-derived scFv used in this study binds to an epitope proximal to the cell membrane.[27] In contrast, PSCA is a relatively small protein, and the scFv used in this study targets an epitope located in the middle region of the extracellular domain (US patent US8404817B2). Despite this difference in the distance of the targeted epitopes to the cell membrane, we observed similar functional trends in PSCA- and HER2-CAR T cells when varying the spacer length. Haso et al. reported that extending the spacer length in CD22-targeted CAR did not enhance binding to a membrane-proximal epitope in CD22,[28] and although the distance of targeted epitopes to the cell membrane may be an important parameter to be considered, epitope accessibility is affected by the structure of targeted proteins and steric hindrance caused by protein-protein interaction.[28,29] Moreover, engineering the spacer domain without major alteration of the spacer length has an impact on epitope binding of CARs and tumor selectivity.[19,27] These studies indicate that the spacer domain must be optimized for each CAR, and also may be affected by functions of other domains, including scFv affinity, transmembrane domain stability, and intracellular co-stimulatory domain activity.

In this study, we found that the HL spacer in PSCA- and HER2-CAR was able to spare cells with low antigen expression. HER2 expression in normal tissues may pose a concern for CAR T cell off-tumor on-target activity, and our results indicate that the HL spacer may be more suitable than the EQ in HER2-CARs to normal tissue toxicities. PSCA expression may be more restricted in normal tissue expression relative to HER2, where a longer spacer length may be used to target tumor cells with lower antigen density. We have also demonstrated that cytokine secretion can be regulated by the spacer domain without affecting antitumor activity. Systemic CAR T cell-derived cytokines can lead to dose-limiting cytokine release syndrome side effects, and using a short spacer such as HL may provide a safer yet comparably effective clinical CAR design. Preclinical studies have demonstrated that IFN-γ secreted by CAR T cells is necessary for remodeling the immune landscape in the solid tumor microenvironment[30–32] and crucial for tumor cell killing in solid tumors.[33] Choosing a long extracellular spacer such as EQ or ΔCH2 in our PSCA- and HER2-CAR may allow for increased IFN-γ secretion critical for eliciting overall antitumor activity against solid tumors. In this study, we evaluated the efficacy of CAR T cells using immunodeficient mouse models with human xenografts. Cytokine release syndrome, which is known to be mediated by monocytes,[34,35] and antitumor function of the endogenous immunity cannot be adequately measured in these murine models that lack the fully functional endogenous immune system. Moreover, IFN-γ signaling regulates $CD8^+$ T cell differentiation and memory phenotypes,[36–38] and repeated antigen stimulation drives T cell effector function and exhaustion.[39,40] We demonstrated that the spacer domain regulates the IFN-γ secretion and activation of CAR T cells, and although we did not evaluate differentiation and memory phenotypes in this study, modifications to the spacer domain may shift the memory/effector composition of CAR T cells and influence overall antitumor activity. Although further studies are warranted, these preclinical data inform on requirements for the extracellular nonsignaling spacer domain of CARs in regulating antitumor activity and tumor antigen selectivity and shed light on engineering CARs to develop potent solid tumor CAR T cells with minimal off-tumor toxicity.

MATERIALS AND METHODS

Cell lines

Human metastatic prostate cancer cell lines DU145 (American Type Culture Collection [ATCC] HTB-81) and PC3 (ATCC CRL-1435) were cultured in RPMI 1640 (Lonza) containing 10% fetal bovine serum (FBS, Hyclone). The human fibrosarcoma cell line HT1080 (ATCC CCL-121), human breast cancer cell line MDA-MB-468 (ATCC HTB-132), and HEK293T (ATCC CRL-3216) were cultured in DMEM (Gibco, 11960-051) containing 10% FBS, 25 mM HEPES (Irvine Scientific, 9319), and 2 mM L-glutamine (Lonza, 17-605E). The human pancreatic cancer cell line HPAC (ATCC CRL-2119) and human breast cancer cell lines MDA-MB-361 (ATCC HTB-27) and MDA-MB-231BR (a kind gift from Dr. Patricia S. Steeg, NIH, Bethesda, MD[41]) were cultured in DMEM:Nutrient Mixture F-12 (DMEM/F12, Life Technologies) containing 10% FBS. The low passage patient-derived breast cancer tumor line (BBM1) generated at City of Hope was cultured in DMEM/F12 containing 10% FBS on 300 mg/mL collagen-coated plates, as previously described.[42] DU145 and PC-3 tumor cells were engineered to express PSCA, and 231BR cells was engineered to express HER2 by lentiviral transduction under the control of the EF1α promoter. To generate PC-3 tumor cells with low PSCA expression, a truncated PGK promoter, PGK100, was used as previously described.[12] Antigen-expressing cells were isolated using the BD FACSAria Special Order Research Product cell sorter, expanded, and frozen in CryoStor CS10 cryopreservation media (BioLife Solutions) until needed for experiments.

DNA constructs and lentivirus production

The PSCA-targeting scFv (A11) sequence was kindly provided by Drs. Anna Wu and Robert Reiter (University of California, Los Angeles), and the HER2-targeting scFv was derived from Herceptin. The intracellular signaling domain of both PSCA- and HER2-CAR constructs contained the co-stimulatory domain of 4-1BB with the CD3ζ cytolytic domain. The transmembrane domain of CD4 and CD8 was used in the PSCA- and HER2-CAR constructs, respectively. The extracellular spacer was altered in the CAR constructs by cloning one of the four spacers: (1) the 229-amino acid-long IgG4 Fc-derived spacer with 2 point mutations in the CH2 domain (L235E; N297Q, abbreviated EQ),[16] (2) the 129-amino acid-long IgG4 Fc-derived spacer with deletion of the CH2 domain (ΔCH2),[16] (3) the 22-amino acid-long IgG4 Fc-derived spacer with deletion of the CH2 and CH3 domains (HL), and (4) the 10-amino acid-long synthetic spacer (L). CAR constructs with a CD19t separated by a T2A ribosomal skip sequence were cloned in an epHIV7 lentiviral backbone.

Lentivirus was manufactured following previously established methods.[12] In short, lentivirus was generated using 293T cells in T-225 flasks and cultured overnight before transfection with packaging plasmids and desired lentiviral backbone plasmid. Supernatants containing lentivirus were collected after 3 to 4 days, filtered, and centrifuged to remove residual cell debris. Lentivirus containing supernatant then underwent incubation with 2 mM magnesium and 25 U/mL Benzonase endonuclease. Suspended lentivirus was then concentrated by high-speed centrifugation (6,080 × *g*) overnight at 4°C. Lentiviral pellets were resuspended in PBS-lactose solution (4 g lactose per 100 mL PBS) and then aliquoted and stored at −80°C. Lentiviral titers were determined by quantifying the expression of CD19t in HT1080 cells.

T cell isolation, lentiviral transduction, and *ex vivo* expansion

Leukapheresis products were obtained from consented research participants (healthy donors) under protocols approved by the City of Hope institutional review board. On the day of leukapheresis, peripheral blood mononuclear cells (PBMCs) were isolated by density gradient centrifugation over Ficoll-Paque (GE Healthcare) followed by multiple washes in PBS/EDTA (Miltenyi Biotec). Cells were rested overnight at room temperature (RT) on a rotator and subsequently washed and resuspended in X-VIVO-15 (Lonza) with 10% FBS (complete X-VIVO). PBMCs were immediately frozen in CryoStor CS5 cryopreservation media (BioLife Solutions) until further processing.

Freshly thawed PBMCs were washed once and cultured in X-VIVO-15 (Lonza) with 10% FBS (complete X-VIVO) containing 100 U/mL recombinant human interleukin-2 (rhIL-2, Novartis Oncology) and 0.5 ng/mL rhIL-15 (CellGenix). For CAR lentiviral transduction, T cells were cultured with CD3/CD28 Dynabeads (Life Technologies), 100 μg/mL protamine sulfate (APP Pharmaceuticals), cytokine mixture (as stated above), and desired lentivirus at a 0.3–1 MOI the day following stimulation. Cells were then cultured in and replenished with fresh complete X-VIVO containing cytokines every 2–3 days. After 7 days, beads were magnetically removed, and cells were further expanded in complete X-VIVO containing cytokines to achieve desired cell yield. CAR T cells were positively selected for CD19t using the EasySep CD19 Positive Enrichment Kit I or II (StemCell Technologies) according to the manufacturer's protocol. Following further expansion, cells were frozen in CryoStor CS5 before *in vitro* functional assays and *in vivo* therapeutic models. Purity and phenotype of CAR T cells were verified by flow cytometry.

Flow cytometry

Fluorophore-conjugated antibodies targeting human CD3 (BD Biosciences, clone: SK7), CD4 (BD Biosciences, clone: SK3), CD8 (BD Biosciences, clone: SK1), CD19 (BD Biosciences, clone: SJ25C1), human CD45 (BD Biosciences, clone: 2D1), CD137 (BD Biosciences, clone: 4B4-1), PD-1 (CD279) (eBiosciences, clone: J105), and mouse CD45 (BioLegend, clone: 30-F11) were used for flow cytometry analysis. The mouse anti-human PSCA antibody (1G8) was kindly provided by Dr. Robert Reiter for detecting PSCA, and biotinylated protein L (GenScript USA) was used for detecting scFv of CARs as previously described.[43] Fluorescent labeled goat anti-mouse Ig (BD Biosciences) and streptavidin (BD Biosciences) secondary antibodies were used for quantifying PSCA and CAR expression, respectively. Cells collected from mice were blocked with rat anti-mouse FcR antibody before staining. Cells were washed and resuspended in buffer (Hank's balanced salt solution without Ca^{2+}, Mg^{2+}, or phenol red, $HBSS^{-/-}$, Life Technologies) containing 2% FBS and 0.5% sodium azide, and incubated with antibodies for 30 min at 4°C in the dark. Cells were washed twice before analysis and staining with secondary antibodies. Cell viability was determined using DAPI (Sigma-Aldrich). Flow cytometry was performed on a MACSQuant Analyzer 10 (Miltenyi Biotec), and the data were analyzed with FlowJo software. CAR T cells were identified by coexpression of CD3 and CD19t, a surrogate marker of transduction, to analyze coculture assays and tissue collected from mice.

In vitro T cell functional assays

CAR T cells and tumor targets were cocultured at indicated E:T ratios with 50,000 target tumor cells (with the exception of HPAC, in which 6,000 target tumor cells were used). T cells and tumor cells were cocultured in X-VIVO containing 10% FBS in the absence of exogenous cytokines in round-bottom 96-well plates for 1–9 days (with media replenishment every 2–4 days). A portion of supernatant from cocultures was collected and frozen for cytokine analysis by ELISA, and cells were analyzed by flow cytometry. To prepare for flow cytometry, the remaining supernatant was transferred to new round-bottom 96-well plates to collect nonadherent cells. Adherent cells were then washed with PBS, lifted by trypsin, and combined with nonadherent cells before staining for flow cytometry as described above. Tumor cell killing by CAR T cells was normalized to UTD T cell conditions.

ELISA

IFN-γ in supernatant was measured using the Human IFNγ ELISA Kit (Invitrogen, 88-7316-88) according to the manufacturer's protocol. Plates were read at 450 nm using Cytation 5 (BioTek).

Animal studies

All of the animal experiments were performed under protocols approved by the City of Hope Institutional Animal Care and Use Committee. A total of 5.0×10^6 respective tumor cells were prepared in $HBSS^{-/-}$ and injected subcutaneously in the flanks of male NSG mice. For the dual tumor study (Figure 5), PC3-PSCA cells were injected in the left flank on day 0, and PC3-$PSCA^{lo}$ cells were injected in the right flank on day 3. Tumor growth was monitored via caliper measurement. When tumors reached 150–250 mm^3, CAR T cells were prepared in PBS and injected i.v. Once tumors reached 15 mm in diameter, mice were euthanized, and tumors were harvested for analysis by immunohistochemistry and flow cytometry. To prepare tumors for flow cytometry, harvested tumors were minced and digested with DNase I and collagenase type D for 30 min at 37°C. Debris was removed through a 70-μm cell strainer, and single-cell suspension was collected. Peripheral blood was collected from isoflurane-anesthetized mice by retro-orbital bleed through heparinized

capillary tubes (Chase Scientific) into polystyrene tubes containing a heparin/PBS solution (1,000 U/mL, Sagent Pharmaceuticals). The volume of blood draw was recorded for cell quantification per microliter of blood. Red blood cells were lysed in single-cell suspension of tumors and peripheral blood using red cell lysis buffer (Sigma-Aldrich) according to the manufacturer's protocol.

Immunohistochemistry

Tumor tissue was fixed for 3 days in 4% paraformaldehyde (Boston BioProducts) and stored in 70% ethanol until further processing. Histology was performed by the Pathology Core at City of Hope. Briefly, paraffin-embedded sections (10 μm) were stained with mouse anti-human CD3 (DAKO). Images were obtained using the Nanozoomer 2.0HT digital slide scanner, and NDP.view2 software (Hamamatsu) was used to determine the area of a tumor section. Fiji (ImageJ) was used to quantify the number of $CD3^+$ human T cells detected by immunohistochemistry to determine the density of $CD3^+$ human T cells per unit area.

Western blotting analysis

Cells were resuspended in RIPA buffer consisting of 25 mM Tris-HCl (pH 8.5), 150 mM NaCl, 1 mM EDTA (pH 8.0), 1% (v/v) NP-40 substitute, 0.5% (w/v) sodium deoxycholate, 0.1% (w/v) SDS, 10 mM NaF, 1 mM NaOV, 10 mM β-glycerophosphate, and 1× Halt Protease and Phosphotase Inhibitor Cocktail (Thermo Scientific). Lysates were incubated on ice for 30 min and then centrifuged at 17,200 × *g* for 20 min at 4°C. Lysate supernatant was transferred to a new tube and analyzed for total protein concentration by bicinchoninic acid assay. Laemmli sample buffer (BioRad) containing DTT (Sigma-Aldrich) was added to proportional quantities of total protein, and samples were boiled at 95°C for 5 min. Protein was electrophoresed on a 12% Criterion TGX Precast Midi Protein Gel (BioRad) using the Criterion Cell (BioRad) and transferred to 0.- nitrocellulose blotting membranes (Genesee) in Tris-glycine transfer buffer (Thermo Scientific) using the Trans-Blot Turbo Electrophoretic Transfer Cell (BioRad). Membranes were washed in deionized water, incubated in Ponceau S solution (Sigma-Aldrich) to confirm protein transfer, and then washed in Tris-buffered saline containing 0.05% Tween 20 (TBST) (Sigma-Aldrich) for 1 min. Membranes were then blocked for 1 h at RT in blocking buffer containing 5% BSA in TBST. After blocking, membranes were transferred to blocking buffer containing mouse anti-human CD3ζ primary antibodies (8D3, BD Biosciences) and incubated overnight at 4°C. Membranes were washed in TBST and then incubated for 45 min at RT in blocking buffer containing horseradish peroxidase-conjugated goat anti-mouse secondary antibody. Membranes were washed in TBST, and images were developed using SuperSignal chemiluminescent substrate (Thermo Scientific).

Statistical analysis

Data are presented as mean ± SEM. Statistical comparisons between groups were performed using the one-way ANOVA with Tukey's multiple comparisons test to calculate p value (*$p < 0.05$, **$p < 0.01$, ***$p < 0.001$). Note that spacers were compared, and UTD T cells were not included in the statistical analyses.

DATA AND CODE AVAILABILITY

The authors confirm that the data supporting the findings of this study are present within the article.

ACKNOWLEDGMENTS

Research reported in this publication was supported by a Prostate Cancer Foundation Young Investigator Award (S.J.P.), PCF Challenge Award (to S.J.F. and S.J.P.), University of California Los Angeles Specialized Program of Research Excellence (P50CA092131), Department of Defense U.S. Army Medical Research Acquisition Activity (to S.J.P., W81XWH-17-1-0208), and a National Comprehensive Cancer Network Young Investigator Award (to S.J.P.). We also thank the Mike and Linda Fiterman Family Foundation for their support. We thank staff members of the Flow Cytometry Core, the Animal Facility Core, the Microscopy Core, and the Pathology Core in the Beckman Research Institute at the City of Hope Comprehensive Cancer Center for excellent technical assistance.

AUTHOR CONTRIBUTIONS

S.J.P., K.T.K., and E.A.G. provided conception and construction of the study. S.J.P., L.A.S., S.J.F., M.S.T., S.L.W., W.-C.C., J.P.M., D.T., B.J., E.A.G., J.G., Y.Y., and K.T.K. provided the design of the experimental procedures, data analysis, and interpretation. K.T.K. and E.A.G. performed the experiments. K.T.K., Y.Y., and S.J.P. wrote the manuscript. S.J.P. supervised the study and is responsible for the overall content. All of the authors reviewed the manuscript.

DECLARATION OF INTERESTS

S.J.P. is a scientific advisor, consultant, and/or receives royalties from Imugene, Mustang Bio, Bayer, Celularity, and Adicet Bio. S.J.F. is a scientific advisor to and receives royalties from Mustang Bio.

REFERENCES

1. Schaft, N. (2020). The Landscape of CAR-T Cell Clinical Trials against Solid Tumors-A Comprehensive Overview. Cancers *12*, 2567.
2. Bagley, S.J., and O'Rourke, D.M. (2020). Clinical investigation of CAR T cells for solid tumors: Lessons learned and future directions. Pharmacol. Ther. *205*, 107419.
3. Mardiana, S., Solomon, B.J., Darcy, P.K., and Beavis, P.A. (2019). Supercharging adoptive T cell therapy to overcome solid tumor-induced immunosuppression. Sci. Transl. Med. *11*, eaaw2293.
4. Mirzaei, H.R., Rodriguez, A., Shepphird, J., Brown, C.E., and Badie, B. (2017). Chimeric Antigen Receptors T Cell Therapy in Solid Tumor: Challenges and Clinical Applications. Front. Immunol. *8*, 1850.
5. Stern, L.A., Jonsson, V.D., and Priceman, S.J. (2020). CAR T Cell Therapy Progress and Challenges for Solid Tumors. Cancer Treat Res. *180*, 297–326.
6. Lynn, R.C., Feng, Y., Schutsky, K., Poussin, M., Kalota, A., Dimitrov, D.S., and Powell, D.J., Jr. (2016). High-affinity FRβ-specific CAR T cells eradicate AML and normal myeloid lineage without HSC toxicity. Leukemia *30*, 1355–1364.
7. Morgan, R.A., Yang, J.C., Kitano, M., Dudley, M.E., Laurencot, C.M., and Rosenberg, S.A. (2010). Case report of a serious adverse event following the administration of T cells transduced with a chimeric antigen receptor recognizing ERBB2. Mol. Ther. *18*, 843–851.
8. Liu, X., Jiang, S., Fang, C., Yang, S., Olalere, D., Pequignot, E.C., Cogdill, A.P., Li, N., Ramones, M., Granda, B., et al. (2015). Affinity-Tuned ErbB2 or EGFR Chimeric Antigen Receptor T Cells Exhibit an Increased Therapeutic Index against Tumors in Mice. Cancer Res. *75*, 3596–3607.

9. Rafiq, S., Hackett, C.S., and Brentjens, R.J. (2020). Engineering strategies to overcome the current roadblocks in CAR T cell therapy. Nat. Rev. Clin. Oncol. *17*, 147–167.
10. Caruso, H.G., Hurton, L.V., Najjar, A., Rushworth, D., Ang, S., Olivares, S., Mi, T., Switzer, K., Singh, H., Huls, H., et al. (2015). Tuning Sensitivity of CAR to EGFR Density Limits Recognition of Normal Tissue While Maintaining Potent Antitumor Activity. Cancer Res. *75*, 3505–3518.
11. Weinkove, R., George, P., Dasyam, N., and McLellan, A.D. (2019). Selecting costimulatory domains for chimeric antigen receptors: functional and clinical considerations. Clin. Transl. Immunol. *8*, e1049.
12. Priceman, S.J., Gerdts, E.A., Tilakawardane, D., Kennewick, K.T., Murad, J.P., Park, A.K., Jeang, B., Yamaguchi, Y., Yang, X., Urak, R., et al. (2018). Co-stimulatory signaling determines tumor antigen sensitivity and persistence of CAR T cells targeting PSCA+ metastatic prostate cancer. OncoImmunology *7*, e1380764.
13. Hamieh, M., Dobrin, A., Cabriolu, A., van der Stegen, S.J.C., Giavridis, T., Mansilla-Soto, J., Eyquem, J., Zhao, Z., Whitlock, B.M., Miele, M.M., et al. (2019). CAR T cell trogocytosis and cooperative killing regulate tumour antigen escape. Nature *568*, 112–116.
14. Priceman, S.J., Tilakawardane, D., Jeang, B., Aguilar, B., Murad, J.P., Park, A.K., Chang, W.C., Ostberg, J.R., Neman, J., Jandial, R., et al. (2018). Regional Delivery of Chimeric Antigen Receptor-Engineered T Cells Effectively Targets HER2(+) Breast Cancer Metastasis to the Brain. Clin. Cancer Res. *24*, 95–105.
15. Majzner, R.G., Rietberg, S.P., Sotillo, E., Dong, R., Vachharajani, V.T., Labanieh, L., Myklebust, J.H., Kadapakkam, M., Weber, E.W., Tousley, A.M., et al. (2020). Tuning the Antigen Density Requirement for CAR T-cell Activity. Cancer Discov. *10*, 702–723.
16. Jonnalagadda, M., Mardiros, A., Urak, R., Wang, X., Hoffman, L.J., Bernanke, A., Chang, W.C., Bretzlaff, W., Starr, R., Priceman, S., et al. (2015). Chimeric antigen receptors with mutated IgG4 Fc spacer avoid fc receptor binding and improve T cell persistence and antitumor efficacy. Mol. Ther. *23*, 757–768.
17. Fujiwara, K., Tsunei, A., Kusabuka, H., Ogaki, E., Tachibana, M., and Okada, N. (2020). Hinge and Transmembrane Domains of Chimeric Antigen Receptor Regulate Receptor Expression and Signaling Threshold. Cells *9*.
18. Muller, Y.D., Nguyen, D.P., Ferreira, L.M.R., Ho, P., Raffin, C., Valencia, R.V.B., Congrave-Wilson, Z., Roth, T.L., Eyquem, J., Van Gool, F., et al. (2021). The CD28-Transmembrane Domain Mediates Chimeric Antigen Receptor Heterodimerization With CD28. Front. Immunol. *12*, 639818.
19. Watanabe, N., Bajgain, P., Sukumaran, S., Ansari, S., Heslop, H.E., Rooney, C.M., Brenner, M.K., Leen, A.M., and Vera, J.F. (2016). Fine-tuning the CAR spacer improves T-cell potency. OncoImmunology *5*, e1253656.
20. Bridgeman, J.S., Hawkins, R.E., Bagley, S., Blaylock, M., Holland, M., and Gilham, D.E. (2010). The optimal antigen response of chimeric antigen receptors harboring the CD3zeta transmembrane domain is dependent upon incorporation of the receptor into the endogenous TCR/CD3 complex. J. Immunol. *184*, 6938–6949.
21. James, S.E., Greenberg, P.D., Jensen, M.C., Lin, Y., Wang, J., Till, B.G., Raubitschek, A.A., Forman, S.J., and Press, O.W. (2008). Antigen sensitivity of CD22-specific chimeric TCR is modulated by target epitope distance from the cell membrane. J. Immunol. *180*, 7028–7038.
22. Wilkie, S., Picco, G., Foster, J., Davies, D.M., Julien, S., Cooper, L., Arif, S., Mather, S.J., Taylor-Papadimitriou, J., Burchell, J.M., and Maher, J. (2008). Retargeting of human T cells to tumor-associated MUC1: the evolution of a chimeric antigen receptor. J. Immunol. *180*, 4901–4909.
23. Hudecek, M., Sommermeyer, D., Kosasih, P.L., Silva-Benedict, A., Liu, L., Rader, C., Jensen, M.C., and Riddell, S.R. (2015). The nonsignaling extracellular spacer domain of chimeric antigen receptors is decisive for in vivo antitumor activity. Cancer Immunol. Res. *3*, 125–135.
24. Guedan, S., Calderon, H., Posey, A.D., Jr., and Maus, M.V. (2019). Engineering and Design of Chimeric Antigen Receptors. Mol. Ther. Methods Clin. Dev. *12*, 145–156.
25. Guest, R.D., Hawkins, R.E., Kirillova, N., Cheadle, E.J., Arnold, J., O'Neill, A., Irlam, J., Chester, K.A., Kemshead, J.T., Shaw, D.M., et al. (2005). The role of extracellular spacer regions in the optimal design of chimeric immune receptors: evaluation of four different scFvs and antigens. J. Immunother. *28*, 203–211.
26. Hudecek, M., Lupo-Stanghellini, M.T., Kosasih, P.L., Sommermeyer, D., Jensen, M.C., Rader, C., and Riddell, S.R. (2013). Receptor affinity and extracellular domain modifications affect tumor recognition by ROR1-specific chimeric antigen receptor T cells. Clin. Cancer Res. *19*, 3153–3164.
27. McComb, S., Nguyen, T., Shepherd, A., Henry, K.A., Bloemberg, D., Marcil, A., Maclean, S., Zafer, A., Gilbert, R., Gadoury, C., et al. (2022). Programmable Attenuation of Antigenic Sensitivity for a Nanobody-Based EGFR Chimeric Antigen Receptor Through Hinge Domain Truncation. Front. Immunol. *13*, 864868.
28. Haso, W., Lee, D.W., Shah, N.N., Stetler-Stevenson, M., Yuan, C.M., Pastan, I.H., Dimitrov, D.S., Morgan, R.A., FitzGerald, D.J., Barrett, D.M., et al. (2013). Anti-CD22-chimeric antigen receptors targeting B-cell precursor acute lymphoblastic leukemia. Blood *121*, 1165–1174.
29. Nagy, P., Friedländer, E., Tanner, M., Kapanen, A.I., Carraway, K.L., Isola, J., and Jovin, T.M. (2005). Decreased accessibility and lack of activation of ErbB2 in JIMT-1, a herceptin-resistant, MUC4-expressing breast cancer cell line. Cancer Res. *65*, 473–482.
30. Yamaguchi, Y., Gibson, J., Ou, K., Lopez, L.S., Ng, R.H., Leggett, N., Jonsson, V.D., Zarif, J.C., Lee, P.P., Wang, X., et al. (2022). PD-L1 blockade restores CAR T cell activity through IFN-γ-regulation of CD163+ M2 macrophages. J. Immunother. Cancer *10*, e004400.
31. Alizadeh, D., Wong, R.A., Gholamin, S., Maker, M., Aftabizadeh, M., Yang, X., Pecoraro, J.R., Jeppson, J.D., Wang, D., Aguilar, B., et al. (2021). IFNγ Is Critical for CAR T Cell-Mediated Myeloid Activation and Induction of Endogenous Immunity. Cancer Discov. *11*, 2248–2265.
32. Gocher, A.M., Workman, C.J., and Vignali, D.A.A. (2022). Interferon-γ: teammate or opponent in the tumour microenvironment? Nat. Rev. Immunol. *22*, 158–172.
33. Larson, R.C., Kann, M.C., Bailey, S.R., Haradhvala, N.J., Llopis, P.M., Bouffard, A.A., Scarfó, I., Leick, M.B., Grauwet, K., Berger, T.R., et al. (2022). CAR T cell killing requires the IFNγR pathway in solid but not liquid tumours. Nature *604*, 563–570.
34. Norelli, M., Camisa, B., Barbiera, G., Falcone, L., Purevdorj, A., Genua, M., Sanvito, F., Ponzoni, M., Doglioni, C., Cristofori, P., et al. (2018). Monocyte-derived IL-1 and IL-6 are differentially required for cytokine-release syndrome and neurotoxicity due to CAR T cells. Nat. Med. *24*, 739–748.
35. Giavridis, T., van der Stegen, S.J.C., Eyquem, J., Hamieh, M., Piersigilli, A., and Sadelain, M. (2018). CAR T cell-induced cytokine release syndrome is mediated by macrophages and abated by IL-1 blockade. Nat. Med. *24*, 731–738.
36. Mazet, J.M., Mahale, J.N., Tong, O., Watson, R.A., Lechuga-Vieco, A.V., Pirgova, G., Lau, V.W.C., Attar, M., Koneva, L.A., Sansom, S.N., et al. (2023). IFNγ signaling in cytotoxic T cells restricts anti-tumor responses by inhibiting the maintenance and diversity of intra-tumoral stem-like T cells. Nat. Commun. *14*, 321.
37. Curtsinger, J.M., Agarwal, P., Lins, D.C., and Mescher, M.F. (2012). Autocrine IFN-γ promotes naive CD8 T cell differentiation and synergizes with IFN-α to stimulate strong function. J. Immunol. *189*, 659–668.
38. Krummel, M.F., Mahale, J.N., Uhl, L.F.K., Hardison, E.A., Mujal, A.M., Mazet, J.M., Weber, R.J., Gartner, Z.J., and Gérard, A. (2018). Paracrine costimulation of IFN-γ signaling by integrins modulates CD8 T cell differentiation. Proc. Natl. Acad. Sci. USA *115*, 11585–11590.
39. Kishton, R.J., Sukumar, M., and Restifo, N.P. (2017). Metabolic Regulation of T Cell Longevity and Function in Tumor Immunotherapy. Cell Metabol. *26*, 94–109.
40. Klebanoff, C.A., Gattinoni, L., Torabi-Parizi, P., Kerstann, K., Cardones, A.R., Finkelstein, S.E., Palmer, D.C., Antony, P.A., Hwang, S.T., Rosenberg, S.A., et al. (2005). Central memory self/tumor-reactive CD8+ T cells confer superior antitumor immunity compared with effector memory T cells. Proc. Natl. Acad. Sci. USA *102*, 9571–9576.
41. Palmieri, D., Bronder, J.L., Herring, J.M., Yoneda, T., Weil, R.J., Stark, A.M., Kurek, R., Vega-Valle, E., Feigenbaum, L., Halverson, D., et al. (2007). Her-2 overexpression increases the metastatic outgrowth of breast cancer cells in the brain. Cancer Res. *67*, 4190–4198.
42. Neman, J., Termini, J., Wilczynski, S., Vaidehi, N., Choy, C., Kowolik, C.M., Li, H., Hambrecht, A.C., Roberts, E., and Jandial, R. (2014). Human breast cancer metastases to the brain display GABAergic properties in the neural niche. Proc. Natl. Acad. Sci. USA *111*, 984–989.
43. Zheng, Z., Chinnasamy, N., and Morgan, R.A. (2012). Protein L: a novel reagent for the detection of chimeric antigen receptor (CAR) expression by flow cytometry. J. Transl. Med. *10*, 29.